

Establishment of an Antibody Specific for AMIGO2 Improves Immunohistochemical Evaluation of Liver Metastases and Clinical Outcomes in Patients with Colorectal Cancer

Keisuke Goto

Tottori University Faculty of Medicine Graduate School of Medicine: Tottori Daigaku Igakubu Daigakuin Igakukei Kenkyuka

Mitsuhiko Osaki

Tottori University Faculty of Medicine Graduate School of Medicine: Tottori Daigaku Igakubu Daigakuin Igakukei Kenkyuka

Runa Izutsu

Tottori University Faculty of Medicine Graduate School of Medicine: Tottori Daigaku Igakubu Daigakuin Igakukei Kenkyuka

Hiroshi Tanaka

Trans Chromosomics, Inc.

Ryo Sasaki

Tottori University Faculty of Medicine Graduate School of Medicine: Tottori Daigaku Igakubu Daigakuin Igakukei Kenkyuka

Akimitsu Tanio

Tottori University Faculty of Medicine Graduate School of Medicine: Tottori Daigaku Igakubu Daigakuin Igakukei Kenkyuka

Hiroyuki Satofuka

Tottori University: Tottori Daigaku

Yasuhiro Kazuki

Tottori University Faculty of Medicine Graduate School of Medicine: Tottori Daigaku Igakubu Daigakuin Igakukei Kenkyuka

Manabu Yamamoto

Tottori University Faculty of Medicine Graduate School of Medicine: Tottori Daigaku Igakubu Daigakuin Igakukei Kenkyuka

Hiroyuki Kugoh

Tottori University Faculty of Medicine Graduate School of Medicine: Tottori Daigaku Igakubu Daigakuin Igakukei Kenkyuka

Hisao Ito

Tottori University Faculty of Medicine Graduate School of Medicine: Tottori Daigaku Igakubu Daigakuin
Igakukei Kenkyuka

Mitsuo Oshimura

Tottori University: Tottori Daigaku

Yoshiyuki Fujiwara

Tottori University Faculty of Medicine Graduate School of Medicine: Tottori Daigaku Igakubu Daigakuin
Igakukei Kenkyuka

Futoshi Okada (✉ fuokada@tottori-u.ac.jp)

Tottori University Faculty of Medicine Graduate School of Medicine: Tottori Daigaku Igakubu Daigakuin
Igakukei Kenkyuka <https://orcid.org/0000-0003-4733-1037>

Short report

Keywords: AMIGO2, Monoclonal antibody, Colorectal cancer, Liver metastasis, Prognosis

Posted Date: October 5th, 2021

DOI: <https://doi.org/10.21203/rs.3.rs-934233/v1>

License:   This work is licensed under a Creative Commons Attribution 4.0 International License.

[Read Full License](#)

Version of Record: A version of this preprint was published at Diagnostic Pathology on January 30th, 2022. See the published version at <https://doi.org/10.1186/s13000-021-01176-2>.

1 **Establishment of an Antibody Specific for AMIGO2**
2 **Improves Immunohistochemical Evaluation of Liver**
3 **Metastases and Clinical Outcomes in Patients with**
4 **Colorectal Cancer**

5
6 Keisuke Goto^{1,2}, Mitsuhiko Osaki^{1,3}, Runa Izutsu¹, Hiroshi Tanaka⁴, Ryo
7 Sasaki¹, Akimitsu Tanio², Hiroyuki Satofuka³, Yasuhiro Kazuki^{3,5}, Manabu
8 Yamamoto², Hiroyuki Kugoh^{3,5}, Hisao Ito¹, Mitsuo Oshimura^{3,4}, Yoshiyuki
9 Fujiwara² and Futoshi Okada^{1,3*}

10
11
12 *Correspondence:

13 Futoshi Okada, Ph.D.

14 Division of Experimental Pathology, Tottori University Faculty of Medicine, 86 Nishicho,
15 Yonago 683-8503, Japan

16 Phone: +81-859-38-6241; Fax: +81-859-38-6240; E-mail: fuokada@tottori-u.ac.jp

17

18

19 ***Abstract***

20 **Instruction:** The human amphoterin-induced gene and open reading frame (AMIGO) was
21 identified as a novel cell adhesion molecule of type I transmembrane protein. AMIGO2 is
22 one of three members of the AMIGO family (AMIGO1, 2, and 3), and the similarity
23 between them is approximately 40% at the amino acid level. We have previously shown that
24 AMIGO2 functions as a driver of liver metastasis. Immunohistochemical analysis of
25 AMIGO2 expression in colorectal cancer (CRC) using a commercially available
26 anti-AMIGO2 mouse monoclonal antibody clone sc-373699 (sc mAb) correlated with liver
27 metastasis and poor prognosis. However, the sc mAb was found to be cross-reactive with all
28 three molecules in the AMIGO family.

29 **Methods:** We generated a rat monoclonal antibody clone rTNK1A0012 (rTNK mAb) for
30 human AMIGO2. The rTNK mAb was used to re-evaluate the association between
31 AMIGO2 expression and liver metastases/clinical outcomes using the same CRC tissue
32 samples previously reported with sc mAb.

33 **Results:** Western blot analysis revealed that a rTNK mAb was identified as being specific
34 for AMIGO2 protein and did not cross-react with AMIGO1 and AMIGO3. The rTNK mAb
35 and sc mAb showed higher AMIGO2 expression, which correlates with a high frequency of
36 liver metastases (65.3% and 47.5%, respectively), while multivariate analysis showed that
37 AMIGO2 expression was an independent prognostic factor for liver metastases ($p =$
38 $7.930E-10$ and $p = 1.707E-5$). The Kaplan-Meier analyses showed that the rTNK mAb ($p =$
39 0.004), but not sc mAb ($p = 0.107$), predicted worse overall survival in patients with high
40 AMIGO2 expression. The relationship between AMIGO2 expression and poor
41 disease-specific survival showed a higher level of significance for rTNK mAb ($p = 0.00004$)
42 compared to sc mAb ($p = 0.001$).

43 **Conclusion:** These results indicate that the developed rTNK1A0012 mAb is an antibody
44 that specifically recognizes AMIGO2 by immunohistochemistry and can be a more reliable
45 and applicable method for the diagnostic detection of liver metastases and worse prognosis
46 in patients with high AMIGO2-expressing CRC.

47 **Keywords:** AMIGO2, Monoclonal antibody, Colorectal cancer, Liver metastasis, Prognosis

48

49 ***Introduction***

50 Cancer survival has improved globally over the last two decades, with an increase in
51 the survival of patients with deadly cancers, such as liver, pancreatic, and lung, by up to 5%
52 (1). The main cause of reduced survival in cancer patients and survivors is distant metastasis
53 rather than growth of the primary tumor, accounting for approximately 90% of
54 cancer-related deaths (2-4). Of the common organs that cause distant metastases, the liver is
55 the most frequent site (59%), except for regional lymph nodes (5). The precise mechanism of
56 metastasis to distant organs, including the liver, that fundamentally undermines cancer
57 therapeutic strategies, is not well-understood (6). Therefore, finding diagnostic biomarkers
58 and therapeutic targets that reliably determine liver metastases is an urgent task.

59 We have identified that AMIGO2, a member of the AMIGO family (AMIGO1, 2, and
60 3), functions as a driver gene for liver metastasis in a mouse model (7). The AMIGO protein
61 was originally identified as a novel cell adhesion molecule that accompanies type I
62 transmembrane proteins containing six leucine-rich repeats and one immunoglobulin-like
63 domain in the extracellular region that are preferentially expressed on fiber tracts of neuronal
64 tissues which participate in axon tract development (8). The three AMIGO family molecules
65 are structurally similar and have shown homophilic and heterophilic binding mechanisms
66 among their molecules; however, the organ expression pattern and biological functions of

67 each protein are independent (9). We found that knocking down AMIGO2 expression, which
68 is highly expressed in liver metastatic tumor cells, reduces the adhesion of tumor cells to
69 hepatic endothelial cells and suppresses liver metastasis. Conversely, it was verified that
70 forced expression of the AMIGO2 gene in non-liver metastatic tumor cells increases the
71 adhesion of tumor cells to hepatic endothelial cells and thereafter forms liver metastases (10).
72 However, AMIGO2-expressing tumor cells did not show increased adhesion to lung
73 endothelial cells and did not affect lung metastases or metastases to other organs. Thus, it
74 was clarified that tumor cells highly expressing AMIGO2 selectively adhere to hepatic
75 endothelial cells expressing AMIGO family molecules by homophilic/heterophilic adhesion
76 patterns to cause liver metastasis (10).

77 Extrapolation of this phenomenon in human cancers has been reported by
78 immunohistochemical staining of AMIGO2 expression in human colorectal cancer (CRC)
79 tissue, which is closely associated with AMIGO2 expression and liver metastasis, but not
80 with lung metastasis and peritoneal dissemination (11). Multivariate analysis showed that
81 AMIGO2 expression in patients with CRC was an independent predictive factor for liver
82 metastasis (11). Furthermore, transcriptionally high levels of AMIGO2 are associated with
83 shortened survival of patients with CRC (11), breast cancer (12), and gastric cancer (13).
84 AMIGO2 has been reported as a novel pathogenesis-related gene in gastric cancer (14),
85 melanoma (15, 16), ovarian cancer (17), and pituitary neuroendocrine tumors (18). In
86 addition, bioinformatics analysis using the transcriptome database selected AMIGO2 as a
87 cancer-related gene candidate for CRC (19), pancreatic cancer (20), and endometrial cancer
88 (21).

89 Most studies have been conducted on the expression of AMIGO2 mRNA in tumor
90 tissues. However, a high expression of AMIGO2 mRNA has been detected in normal tissues,
91 and is most prominent in the cerebellum, retina, liver, and lung (9). Lower but steady

92 AMIGO2 expression is also found in the cerebrum, kidneys, small intestine, spleen, and
93 testis (9). These physiological conditions indicate that as long as AMIGO2 expression is
94 assessed as tissue-wide mRNA expression, its association with carcinogenesis in each organ
95 cannot be determined. Therefore, immunohistochemical staining is the most reliable method
96 for accurately evaluating AMIGO2 expression in cancerous tissues. For this purpose, we
97 have analyzed AMIGO2 expression by using commercially available anti-AMIGO2 mouse
98 monoclonal antibody (sc-373699); however, we noticed that the antibody recognizes
99 AMIGO1 and AMIGO3 as well as AMIGO2. We also investigated the specificity of three
100 commercially available affinity purified polyclonal antibodies. These antibodies were also
101 recognized as AMIGO family molecules.

102 In this study, we developed a new AMIGO2-specific antibody that does not react with
103 AMIGO1 and AMIGO3, and compared the efficacy of the new antibody using the same
104 tissue samples that previously reported a significant correlation between AMIGO2
105 expression in primary CRC tissue and liver metastasis (11).

106

107 ***Materials and Methods***

108 **Cell Culture and Transfection**

109 P3X63Ag8.653 myeloma cells (CRL-1580) and HepG2 hepatocellular carcinoma cells
110 (HB-8065) were purchased from the American Type Culture Collection (ATCC, Manassas,
111 VA). P3X63Ag8.653 cells and HepG2 cells were respectively maintained in RPMI-1640
112 medium (05911; Nissui Pharmaceutical, Tokyo, Japan) and Dulbecco's modified Eagle's
113 medium (05919; Nissui Pharmaceutical) containing 10% heat-inactivated fetal bovine serum
114 (FBS, F7524, Sigma-Aldrich, St. Louis, MO) and L-glutamine. The cell lines were
115 maintained at 37°C in a humidified 5% CO₂/95% air mixture.

116 Expression plasmids for human AMIGO1 (pEZ-M02/AMIGO1), AMIGO2
117 (pEZ-M02/AMIGO2), and AMIGO3 (pEZ-M02/AMIGO3) were purchased from
118 GeneCopoeia (EX-E1371-M02, EX-E1271-M02, EX-E1133-M02, Rockville, MD). The
119 pEZ-M02 vector was used as the control plasmid. HepG2 cells were transfected with these
120 plasmids using Lipofectamine 2000 reagent (12566014, Thermo Fisher Scientific, Waltham,
121 MA) according to the manufacturer's instructions. Transfectants stably expressing the
122 introduced vector plasmid were selected by continuous neomycin treatment at 450 $\mu\text{g/mL}$
123 (10131035, Thermo Fisher Scientific). Neomycin-resistant cells were cloned by the limiting
124 dilution method and maintained in a medium containing neomycin.

125

126 **Antigens**

127 To produce an antigen for immunization, a DNA fragment of AMIGO2 extracellular
128 domain (NM_001143668) was amplified by PCR using primers (forward: 5'-GCG AAG
129 CTT GTG TGC CCC ACC GCT TGC AT-3' and reverse: 5'-GCG CTC GAG TGT GTT
130 AAA TGC CTC ATG AGC ATG GG-3'), and was subcloned into pET-32b(+) (69016,
131 Sigma-Aldrich) using *Hind*III and *Xho*I restriction enzymes (resulting in
132 pET32b-AMIGO2-EX). AMIGO2-EX protein was difficult to express in *Escherichia coli*
133 Rosseta-gami B (DE3) pLysS (71137, Merck KGaA, Darmstadt, Germany).
134 pET32b-AMIGO2-EX was digested with *Eco*RI (an *Eco*RI site is located near the upstream
135 end of the leucine-rich repeat sequence), blunted using Blunting high, and then digested with
136 *Eco*RV (at a site upstream of AMIGO2-EX) to eliminate its leucine-rich repeat sequence.
137 Therefore, this vector consisted of the Ig-like domain of AMIGO2 (named
138 pET32b-AMIGO2-Ig) and produces the Trx-AMIGO2-Ig recombinant protein. To obtain the
139 GST-AMIGO2-Ig recombinant fusion protein, pGEX-6P-1 (28954648, GE Healthcare,

140 Chicago, IL) was modified by inserting the synthesized DNA (5'-ACG AGA TCT GCC
141 ATG GAC AAG CTT GTC GAC ACG AGC TCG AAT TCG GAT CCC CCG GGG CTC
142 GAG CAC CAC CAC CAC CAC TGA GCT GAG CGG CCG CTC A-3') using *Bgl*II
143 and *Not*I restriction enzymes (resulting in pGEX-MCS-His). The amplified AMIGO2-Ig
144 fragment was also cloned into pGEX-MCS-His. Restriction enzymes and DNA-modifying
145 enzymes were purchased from New England Biolabs (Ipswich, MA) and Toyobo (Tokyo,
146 Japan), respectively. Primers were ordered from Eurofins (Huntsville, AL). *E. coli* strain
147 (DH5 α) competent cells were obtained from Takara Bio (9057, Shiga, Japan).

148 After transformation of *E. coli* gami B pLysS (DE3) with each vector, the recombinant
149 proteins were expressed by induction with 1.0 mM isopropyl- β -D (-)-thiogalactopyranoside
150 (094-05144, Fujifilm Wako Pure Chemical, Osaka, Japan) in a LB medium. Transformation
151 using the empty vector, pET-32b(+) was also carried out to produce the Tag protein for use
152 in hybridoma screening as a negative control. After harvesting the cells and sonication, the
153 recombinant proteins were obtained as inclusion bodies. Following solubilization with 6 M
154 guanidine hydrochloride (078-05003, Fujifilm Wako Pure Chemical) in PBS with 0.1 mM
155 glutathione (oxide form, 078-03333, Fujifilm Wako Pure Chemical) and 1 mM glutathione
156 (redox form, 077-02011, Fujifilm Wako Pure Chemical), recombinant protein was purified
157 using Ni-NTA columns (30410, Qiagen, Hulsterweg, Venlo, Netherlands) with elution using
158 100 mM imidazole (091-00012, Fujifilm Wako Pure Chemical) containing 6 M guanidine
159 hydrochloride. After dialyzing the eluted fraction against PBS containing 0.4 M arginine
160 (PBS-A, 091-04611, Fujifilm Wako Pure Chemical), samples were diluted to about 1 mg/mL
161 and stored at -30°C.

162

163 **Immunization**

164 Protein antigens were prepared in PBS or in PBS-A at 1 mg/mL, and the volume
165 corresponding to the desired amount of protein was increased to an injectable volume with
166 PBS or PBS-A. This volume was then mixed 1:1 (v/v) with either Freund's adjuvant,
167 complete (F5881, Sigma-Aldrich), or Sigma adjuvant system (S6322, Sigma-Aldrich). For
168 viscous adjuvants, the solution was mixed by repeated passage through a syringe until a
169 smooth emulsion was formed (over approximately 30 min on ice). Injections were performed
170 on 6-week-old male and female Jcl:Wistar rats (Clea, Tokyo, Japan) using a 1 mL glass
171 syringe and a 27-gauge needle. Prime and boost injections of 250 μ g protein were injected
172 intraperitoneally every two weeks. Final boosts of 250 μ g of protein were delivered
173 intravenously without adjuvant via the tail vein. Volumes varied depending on the injection
174 route and experimental requirements and were in accordance with the relevant JP Home
175 Office animal license for the procedure. The experimental protocol was approved by the
176 Committee of the Institute for Animal Experimentation of Tottori University (17-Y-28).

177

178 **Hybridoma Generation**

179 After confirming induction of serum antibodies against AMIGO2-Ig protein, spleens
180 and lymph nodes from immunized rats were harvested from euthanized rats, homogenized to
181 single-cell suspensions, and fused with myeloma P3X63Ag8.653 cells using an
182 electro-cell-fusion generator (ECFG21; Nepagene, Chiba, Japan). Fused hybridoma cells
183 were plated in 96-well plates. After approximately 14 days of culture, a primary screen of
184 supernatants was performed by ELISA. Hybridoma clones producing AMIGO2-specific Abs
185 were identified by ELISA using GST-AMIGO2-Ig following HAT selection. Positive wells
186 were picked and passaged in 96-well plates. Each supernatant was reanalyzed by ELISA
187 using Tag, Trx-AMIGO2-Ig, and GST-AMIGO2-Ig. Hybridoma clones that reacted with

188 Trx-AMIGO2-Ig and GST-AMIGO2-Ig, but not Tag, were established using two or more
189 limited dilutions.

190

191 **Hybridoma Screening**

192 Hybridoma cells producing AMIGO2-specific mAb were identified using ELISA. In
193 brief, a 96-well immunoassay plate (44-2404, Thermo Fisher Scientific) were coated with 50
194 $\mu\text{g}/\text{well}$ antigen, washed three times with PBS-T (0.05% v/v Tween-20: 160-21211, Fujifilm
195 Wako Pure Chemical), and blocked with PBS containing 5% skim milk (232100, Difco,
196 Detroit, MI) for 30 min. After incubation with 100 μL of serially diluted serum samples or
197 supernatant for 1 h, plates were again washed and incubated with 100 μL of anti-rat IgG
198 (H+L)-HRP conjugate (A110-105P, Bethyl Laboratories, Montgomery, TX) diluted
199 50,000-fold in TBS-T (50 mM Tris-HCl, pH 8.0) (T1503, Sigma-Aldrich), 150 mM NaCl
200 (195-01663, Fujifilm Wako Pure Chemical), 0.05% v/v Tween 20) for 30 min. Plates were
201 washed again as described above, developed using 100 μL of *o*-phenylenediamine
202 (160-11022, Fujifilm Wako Pure Chemical) for 30 min, and stopped using 25 μL of 1 M
203 H_2SO_4 (95626-06, Nacalai Tesque, Kyoto, Japan). Absorbance was measured at 492 nm by
204 microplate reader Epoch2 (Bio Tek, Winooski, VT).

205

206 **Western Blotting**

207 Cells were washed in cold PBS and lysed in lysis buffer containing 20 mM Tris-HCl
208 (pH 7.4), 150 mM NaCl, 0.1% sodium dodecyl sulfate (SDS), 1% sodium deoxycholate, 1%
209 Triton X-100, 1 $\mu\text{g}/\text{mL}$ aprotinin, and 1 $\mu\text{g}/\text{mL}$ leupeptin. Lysates were centrifuged at
210 15,000 rpm for 5 min. Protein concentrations were estimated using the Bradford protein
211 assay (5000006, Bio-Rad Laboratories, Hercules, CA) with bovine serum albumin as the

212 standard. The cell lysate was incubated with or without PNGase F (P0704S, New England
213 Biolabs, UK) at 37°C for 1 h.

214 Proteins were resolved by SDS-polyacrylamide gel electrophoresis using 10% gels,
215 followed by electrotransfer to polyvinylidene difluoride membranes (ISEQ00010, Millipore,
216 Bedford, MA). The membranes were then blotted using primary antibodies, washed, then
217 incubated with secondary antibodies. The membranes were washed, and the bound
218 antibodies were detected using an enhanced chemiluminescence detection system
219 (GERPN2209, Amersham, Buckinghamshire, UK). The anti-AMIGO2 primary antibodies
220 used in this study were rTNK1A0012; sc-373699, Santa Cruz Biotechnology, Dallas, TX;
221 LS-C404504, LifeSpan BioSciences, Seattle, WA; #36094, Signalway Antibody, College
222 Park, MD; HPA054004, Sigma-Aldrich), and anti- β -actin (1:2000; A1978, Sigma-Aldrich).
223 The secondary antibodies used in this study were as follows: anti-mouse IgG-HRP
224 (PM009-7, MBL, Nagoya, Japan), anti-rabbit IgG-HRP (458, MBL, Nagoya, Japan), and
225 goat anti-rat IgG-HRP pre-adsorbed (ab98425, Abcam, Cambridge, UK).

226

227 **Patient Samples**

228 Immunohistochemical analysis was performed using paraffin-embedded colorectal
229 cancer samples from 173 patients who underwent proctocolectomies at Tottori University
230 Hospital between January 2007 and December 2015. For 173 cases, excluding the samples
231 that were no longer available, the same samples reported in the previously were used (11).
232 Clinicopathological findings were determined using the Japanese classification of colorectal
233 carcinoma (16). None of the patients had received radiotherapy, chemotherapy, or other
234 medical interventions before surgery.

235

236 **Immunohistochemistry**

237 Tissue samples were fixed in formalin and embedded in paraffin. Serial sections were
238 cut at 4 μm , deparaffinized in xylene, and rehydrated using a graded alcohol series. For
239 retrieval of AMIGO2, the sections were heated at 121°C for 20 min in an autoclave in 10
240 mM citrate buffer (pH 6.0). The samples were incubated in 0.1% hydrogen peroxidase for 15
241 min to block endogenous peroxidases and in 10% normal goat serum (424041, Nichirei
242 Biosciences, Tokyo, Japan) for 15 min to prevent non-specific antigen binding. The slides
243 were subsequently incubated with primary antibodies (rTNK1A0012a) overnight at 4°C,
244 then incubated with goat anti-rat IgG-HRP for 20 min. Staining was visualized with
245 diaminobenzidine (SK-4105, Vector Laboratories, Burlingame, CA), and the sections were
246 counterstained with hematoxylin. The expression of AMIGO2 in CRC cells was evaluated in
247 a blinded manner. In brief, five fields were chosen at random and examined at $\times 400$
248 magnification. The intensity of immunoreactivity was bisected according to a previous report
249 (11), and the staining intensity of the primary CRC was defined as low (< 30% staining
250 intensity) and high (\geq 30% staining intensity).

251

252 **Statistical Analysis**

253 All statistical analyses were performed using SPSS version 25 software (IBM Japan,
254 Toyo, Japan). The χ^2 tests were used to compare the clinicopathological characteristics of
255 tumors with high and low AMIGO2 expression. Univariate and multivariate analyses for the
256 identification of prognostic factors for overall survival were carried out using the Cox
257 proportional hazard regression model, and identification of prognostic factors for liver
258 metastases were carried out using the logistic regression model. Kaplan-Meier survival

259 curves were plotted and compared using a generalized log-rank test. Statistical significance
260 was set at $p < 0.05$. Where appropriate, data are expressed as mean \pm SD.

261

262 ***Results***

263 **Evaluation of Reactivity of Monoclonal Antibody (rTNK1A0012) Against**

264 **Human AMIGO2 Protein**

265 We developed rat monoclonal antibodies against the extracellular domain of human
266 AMIGO2 for use in clinical diagnosis. The monoclonal antibodies with high
267 immunoglobulin titers were selected by enzyme-linked immunosorbent assay (ELISA) (data
268 not shown; An additional file shows this in more detail [see Additional file 1]). Of the 19
269 candidate antibodies, the monoclonal antibody clone rTNK1A0012 (rTNK mAb) was
270 established to detect human AMIGO2 for further study.

271 To evaluate whether the rTNK mAb reacted specifically with human AMIGO2,
272 HepG2 cells were transfected with a plasmid containing AMIGO1, AMIGO2, or AMIGO3
273 gene, and established stably expressing cell lines. Western blot analysis showed that rTNK
274 mAb was reactive with AMIGO2 (HepG2-A2), while the rTNK mAb did not react with the
275 other AMIGO family molecules; that is, AMIGO1 (HepG2-A1), AMIGO3 (HepG2-A3), or
276 empty vector-transfected cells (HepG2-E) (Figure 1A). The rTNK mAb was found to be
277 highly specific and sensitive to human AMIGO2. The same protein lysates obtained from the
278 transfectants of the AMIGO family molecules were used to examine the specificity of the
279 commercially available mouse anti-human AMIGO2 monoclonal antibody (sc-373699, sc
280 mAb). On the other hands, the sc mAb cross-reacted with all types of AMIGO family
281 molecules (Figure 1B). Next, we investigated the specificity of three commercially available

282 polyclonal antibodies (LS-C404504, #36094, and HPA054004). However, these antibodies
283 were recognized as all AMIGO family molecules (Figure 2).

284 In addition to the predicted molecular weight of human AMIGO2 based on the amino
285 acid sequence of 58 kDa (22), multiple/diffuse bands suggest that the AMIGO2 protein may
286 undergo a series of post-translational modifications such as glycosylation (23). Since there
287 are two main types of protein glycosylation, *N*-glycosylation and *O*-glycosylation (24), the
288 peptide-*N*-glycosidase F (PNGase F), which cleaves *N*-linked oligosaccharides (25), was
289 used first. Treatment of HepG2-A2 cell lysates with PNGase F caused a shift in
290 electrophoretic mobility and resulted in conversion of the multiple/diffuse band to a single
291 band (Figure 1C). In contrast, treatment of HepG2-A2 cell lysates with alkaline
292 β -elimination, which releases *O*-linked glycans from *N*-glycosylated proteins (24), did not
293 cause any shift in electrophoretic mobility (Figure 1D). This indicates that the AMIGO2
294 protein is not *O*-glycosylated. It was clarified that the human AMIGO2 protein may undergo
295 *N*-glycosylation as a post-translational modification but may not undergo *O*-glycosylation.

296

297 **Immunohistochemical Detection of AMIGO2 Expression by rTNK mAb** 298 **and Clinicopathologic Risk Factors**

299 The efficacy of the rTNK mAb against AMIGO2 was re-evaluated using the same
300 CRC tissue as previously reported by immunohistochemical staining with the commercially
301 available sc mA (11). We performed immunohistochemistry of AMIGO2 in 173 CRC tissue
302 samples. AMIGO2 was mainly expressed in tumor cells and was rarely expressed in the
303 stroma (Figure 3). AMIGO2 was located in both the cytoplasm and nucleus of the tumor
304 cells (Figure 3B and 3D). The expression of AMIGO2 was quantified using a visual grading
305 system based on the extent of staining. The cut-off value for AMIGO2 expression was

306 determined as the staining intensity of the primary CRC at 30%, as in a previous report (11),
307 and the cases were divided into two groups: high and low expression. High expression was
308 defined as an AMIGO2-positive tumor cell proportion of 30% or higher ($\geq 30\%$, Figure 3B
309 and 3D). On the other hand, low expression was defined as less than 30% of positive tumor
310 cells ($< 30\%$, Figure 3A and 3C).

311 Of the 173 tumor specimens evaluated, 28.3% (49/173) had AMIGO2 high expression,
312 while 71.7% (124/173) had AMIGO2 low expression (Table 1). To evaluate the prognostic
313 value of AMIGO2, we analyzed the correlations between clinicopathological variables and
314 the expression of AMIGO2 in tumor tissues (Table 1 and Figure 4). A high expression of
315 AMIGO2 (32/49; 65.3%) was more closely associated with liver metastasis than low
316 AMIGO2 expression (17/124; 13.7%) ($p = 1.15E-11$; Figure 4A). Patients with high
317 AMIGO2-expression tumors were found to be more likely to develop lung metastases (5/49;
318 10.2%) than patients with low expression tumors (3/124; 2.4%) ($p = 0.042$; Figure 4B),
319 whereas AMIGO2 expression was found to be independent of peritoneal dissemination (high
320 2/49, 4.1% vs. low 4/124, 3.2%; $p = 0.546$; Figure 4C). There was no significant correlation
321 between AMIGO2 expression and age, sex, tumor location, tumor size, histological grade,
322 depth of invasion, lymph node metastasis, lymphatic invasion, and vascular invasion (Table
323 1).

324

325 **Improved Correlation between AMIGO2 Expression Detected by rTNK1** 326 **mAb and Liver Metastasis and Poor Prognosis**

327 In an univariate Cox regression analysis for different established risk factors for CRC,
328 in addition to AMIGO2 expression ($p = 0.005$), age ($p = 0.006$) and vascular invasion ($p =$
329 0.019) were also associated with poor overall survival (Table 2). To compare the

330 independent predictive value of AMIGO2 status for overall survival, a multivariate analysis
331 with Cox's proportional hazard regression model was performed. This analysis revealed that
332 AMIGO2 status ($p = 0.022$), age ($p = 0.007$), and vascular invasion ($p = 0.029$) had an
333 independent prognostic impact (Table 2). Of particular interest was whether AMIGO2
334 expression added any predictive value as a widely used prognostic factor for liver metastasis
335 in CRC. Multivariate logistic regression analysis showed that the risk factors for liver
336 metastases were significantly higher in patients with AMIGO2 high-expressing CRC than in
337 those with AMIGO2 low-expressing tumors ($p = 7.930E-10$, Table 3).

338 A Kaplan-Meier survival analysis was performed to compare which of the two
339 anti-AMIGO2 monoclonal antibodies could more accurately determine the clinically worse
340 outcome of CRC patients based on AMIGO2 expression levels. Overall survival tended to
341 have a poor prognosis in patients with high AMIGO2 levels (Figure 5A). Most notably, in an
342 analysis, rTNK mAb ($p = 0.004$), but not sc mAb ($p = 0.107$), predicted worse overall
343 survival in patients with high AMIGO2 expression than in those with low AMIGO2
344 expression (Figure 5A). Moreover, a high expression of AMIGO2 resulted in short
345 disease-specific survival, which is common to both antibodies, but rTNK mAb ($p =$
346 0.000044) was detected at a significantly higher level compared to sc mAb ($p = 0.001$;
347 Figure 5B).

348 The above findings showed that immunohistochemical detection of high AMIGO2
349 expression in CRC patients with rTNK mAb serves as a superior diagnostic biomarker and
350 allows for prediction of poor prognoses by detecting liver metastasis compared to
351 commercially available antibodies.

352

353 ***Discussion***

354 In this study, we produced a rat rTNK mAb specific for human AMIGO2, and
355 confirmed that it detects AMIGO2 but does not cross-react with other AMIGO family
356 molecules; that is, AMIGO1 and AMIGO3. By comparing the results previously reported for
357 commercially available sc mAb with rTNK mAb using the same CRC tissues, the following
358 five new facts and the usefulness of rTNK mAb were clarified: (i) the detection rate of liver
359 metastases in CRC patients with high AMIGO2 expression in primary tumors improved
360 from 47.5% for sc mAb (11) to 65.3% for rTNK mAb (Figure 4A); (ii) the association
361 between AMIGO2 expression and liver metastasis by multivariate analysis resulted in
362 predictability with sc mAb ($p = 1.707E-5$) (11); but it was significantly predictable with
363 rTNK mAb ($p = 7.930E-10$, Table 3); (iii) AMIGO2 expression and overall survival were not
364 statistically significant when detected with sc mAb ($p = 0.107$), but was significantly
365 correlated with worse prognosis when detected with rTNK mAb ($p = 0.004$, Figure 5A); (iv)
366 in disease-specific survival, high AMIGO2 expression resulted in a poor prognosis, which
367 can also be detected with sc mAb ($p = 0.001$), whereas it had a much higher correlation with
368 rTNK mAb ($p = 0.000044$, Figure 5B); and (v) factors affecting liver metastasis in
369 multivariate logistic regression analysis using sc mAb were AMIGO2 expression ($p =$
370 $1.707E-5$), lymph node metastasis, vascular invasion, and sex (11). In contrast, analysis
371 using rTNK mAb eliminated the risk of lymph node metastasis and vascular invasion,
372 leaving only AMIGO2 expression ($p = 7.930E-10$) and sex ($p = 0.049$). The above findings
373 showed that by using rTNK mAb, AMIGO2 expression serves as a superior prognostic
374 immunohistochemical biomarkers, especially for the detection of liver metastases and worse
375 prognosis in CRC patients, compared to commercially available sc mAb.

376 Intriguingly, the use of rTNK mAb revealed that the AMIGO2 protein was
377 *N*-glycosylated. Since it has been reported that the AMIGO1 protein, which is mainly
378 expressed in the central nervous system, is *N*-glycosylated (26), the AMIGO family proteins

379 may be included in those proteins in which half of all mammalian proteins are glycosylated
380 as post-translational modifications (27). In tumor tissues, abnormal glycosylation, that is,
381 alterations to glycan epitopes, such as truncated *O*-glycans; altered *N*-glycan branching;
382 increased sialylation; and fucosylation have been observed (23, 28-30). These specific
383 glycosylations have been shown to accelerate malignancies in tumor cells, such as signal
384 transduction (31), growth (32), tumor immunity (33), epithelial-mesenchymal transition (34),
385 motility (31), and metastasis (35), especially in CRC (36). As a typical example of
386 glycosylation-mediated liver metastasis in CRC patients, primary tumors expressing sialyl
387 Lewis^x (sLe^x) specifically bind or adhere to activated hepatic vascular E-selectin (31, 37-39).
388 We believed that CRC cells expressing AMIGO2 selectively form liver metastases by
389 specifically binding to hepatic endothelial cells expressing AMIGO family molecules in a
390 homophilic/heterophilic manner. To comprehensively understand the mechanism of liver
391 metastasis due to AMIGO2 expression, it is necessary to examine how *N*-glycosylation of
392 the AMIGO2 protein is associated with liver metastasis. Since there are eight putative
393 *N*-glycosylation sites at 58, 104, 281, 288, 345, 373, 381, and 384 asparagine residues (22)
394 in AMIGO2 that undergo *N*-glycosylation, we are going to investigate the degree of these
395 *N*-glycosylation and liver metastatic activity.

396 In conclusion, we succeeded in establishing a monoclonal antibody that specifically
397 recognizes human AMIGO2 and demonstrated its clinical applicability by
398 immunohistochemistry. Expression of AMIGO2 by rTNK mAb may be a promising tool for
399 predicting liver metastasis and poor prognosis in CRC patients.

400

401 **List of abbreviations**

402 AMIGO, amphoterin-induced gene and open reading frame, CRC, colorectal cancer; mAb,
403 monoclonal antibody; sc mAb, anti-AMIGO2 mouse monoclonal antibody clone sc-373699;
404 rTNK mAb, anti-AMIGO2 rat monoclonal antibody clone rTNK1A0012.

405

406 ***Declarations***

407 **Ethics approval and consent to participate**

408 The experimental protocol was conducted according to the guidelines of the Declaration of
409 Helsinki, approved by the Tottori University Hospital Institutional Review Board (ID:
410 17A142 on June 26, 2018), and approved by the Committee of the Institute for Animal
411 Experimentation of Tottori University (ID: 17-Y-28 on September 11, 2017).

412

413 **Consent for publication**

414 Not applicable.

415

416 **Availability of data and materials**

417 All data generated or analyzed during this study are included in this published article.

418

419 **Competing interests**

420 MOsh is a CEO, employee and shareholder of Trans Chromosomics, Inc. HT is employees of
421 Trans Chromosomics, Inc. The other authors declare no financial or other interests regarding
422 this manuscript that might be construed as a conflict of interest.

423

424 **Funding**

425 This work was supported in part by a Grant-in-Aid for Scientific Research C to FO
426 (20K07447), a Grant-in-Aid for Early-Career Scientists to AT (20K16303) from the
427 Japanese Ministry of Education, Culture, Sports, Science and Technology, CREST from
428 Japan Science and Technology Agency to YK (JPMJCR18S4), and Basis for Supporting
429 Innovative Drug Discovery and Life Science Research of Japan Agency for Medical
430 Research and Development to YK (JP21am0101124).

431

432 **Authors' contributions**

433 KO, MOsa, RI, HI performed immunohistochemistry and quantification; RI, RS performed
434 *in vitro* experiments and biochemical analysis; KO wrote original draft; HT, HS, YK, HK,
435 MOsh designed & arranged generation of monoclonal antibodies; KO, MOsa, MY, YF, FO
436 contributed to formulation of the experimental design; KO, AT, MY YF performed statistical
437 analysis; KO, MOsa, RI, AT, HS, YK, MY, HK, HI, MOsh, YF, FO contributed to
438 interpretation and discussion of the results; FO designed & arranged the whole experiments,
439 and wrote the manuscript. The authors read and approved the final manuscript.

440

441 **Acknowledgements**

442 We would like to thank Yukako Sumida, Eri Kaneda, and Genki Hichiwa at Tottori
443 University, and Toko Kurosaki, Michika Fukino, Maya Hiratsuka, Masami Morimura, Maki
444 Takami, Kazuhisa Honma, Haruka Takayama and Shoko Takehara at Trans Chromosomics
445 Inc. for their technical support. This research was partly performed at the Tottori Bio Frontier
446 managed by Tottori prefecture and Tottori Pharmaceutical Innovation Center managed by
447 Chromosome Engineering Research Center, Tottori University.

448

449 **Authors' information**

450 ¹Division of Experimental Pathology, Tottori University Faculty of Medicine, Yonago
451 683-8503, Japan. ²Division of Gastrointestinal and Pediatric Surgery, Tottori University
452 Faculty of Medicine, Yonago 683-8503, Japan. ³Chromosome Engineering Research Center
453 (CERC), Tottori University, Yonago 683-8503, Japan. ⁴Trans Chromosomics, Inc., Yonago,
454 Tottori 683-8503, Japan. ⁵Division of Genome and Cellular Functions, Tottori University
455 Faculty of Medicine, Yonago 683-8503, Japan.

456

457 ***References***

- 458 1. Allemani C, Matsuda T, Carlo VD, Harewood R, Matz M, Nikšić M, et al. Global
459 surveillance of trends in cancer survival 2000–14 (CONCORD-3): Analysis of
460 individual records for 37 513 025 patients diagnosed with one of 18 cancers from 322
461 population-based registries in 71 countries. *Lancet*. 2018;391:1023-75.
462 [https://doi.org/10.1016/S0140-6736\(17\)33326-3](https://doi.org/10.1016/S0140-6736(17)33326-3).
- 463 2. Lambert AW, Pattabiraman DR, Weinberg RA. Emerging biological principles of
464 metastasis. *Cell*. 2017;168: 670-91. <https://doi.org/10.1016/j.cell.2016.11.037>.
- 465 3. Li F, Tiede B, Massague J, Kang Y. Beyond tumorigenesis: cancer stem cells in
466 metastasis. *Cell Res*. 2007;17:3–14. <https://doi.org/10.1038/sj.cr.7310118>.
- 467 4. Talmadge JE, Fidler IJ. AACR centennial series: the biology of cancer metastasis:
468 historical perspective. *Cancer Res*. 2010;70:5649-69.
469 <https://doi.org/10.1158/0008-5472.CAN-10-1040>.
- 470 5. Budczies J. et al. The landscape of metastatic progression patterns across major human
471 cancers. *Oncotarget*. 2015;6:570-83. <https://doi.org/10.18632/oncotarget.2677>.
- 472 6. Abyadeh M, Meyfour A, Gupta V, Moghaddam MZ, Fitzhenry MJ, Shahbazian S, et al.

- 473 Recent advances of functional proteomics in gastrointestinal cancers- a path towards the
474 identification of candidate diagnostic, prognostic, and therapeutic molecular biomarkers.
475 *Int J Mol Sci.* 2020;21:8532. <https://doi.org/10.3390/ijms21228532>.
- 476 7. Sung H, Ferlay J, Siegel RL, Laversanne M, Soerjomataram I, Jemal A, et al. Global
477 cancer statistics 2020: GLOBOCAN estimates of incidence and mortality worldwide for
478 36 cancers in 185 countries. *CA Cancer J Clin.* 2021;71:209-49.
479 <https://doi.org/10.3322/caac.21660>.
- 480 8. Abdalla EK, Adam R, Bilchik AJ, Jaeck D, Vauthey JN, Mahvi D. Improving
481 resectability of hepatic colorectal metastases: Expert consensus statement. *Ann Surg
482 Oncol.* 2006;13:1271-80. <https://doi.org/10.1245/s10434-006-9045-5>.
- 483 9. Kuja-Panula J, Kiiltomäki M, Yamashiro T, Rouhiainen A, Rauvala H. AMIGO, a
484 transmembrane protein implicated in axon tract development, defines a novel protein
485 family with leucine-rich repeats. *J Cell Biol.* 2003;160:963-73. [https://doi:
486 10.1083/jcb.200209074](https://doi:10.1083/jcb.200209074).
- 487 10. Kanda Y, Osaki M, Onuma K, Sonoda A, Kobayashi M, Hamada J, et al. Amigo2
488 upregulation in tumour cells facilitates their attachment to liver endothelial cells
489 resulting in liver metastases. *Sci Rep.* 2017;7:43567. <https://doi.org/10.1038/srep43567>.
- 490 11. Tanio A, Saito H, Amisaki M, Hara K, Sugezawa K, Uejima C, et al. AMIGO2 as a
491 novel indicator of liver metastasis in patients with colorectal cancer. *Oncol Lett.* 2021;
492 21:278. <https://doi.org/10.3892/ol.2021.12539>.
- 493 12. Sonzogni O, Haynes J, Seifried LA, Kamel YM, Huang K, BeGora MD, et al. Reporters
494 to mark and eliminate basal or luminal epithelial cells in culture and in vivo. *PLoS Biol.*
495 2018;16:e2004049. <https://doi.org/10.1371/journal.pbio.2004049>
- 496 13. Nakamura S, Kanda M, Shimizu D, Tanaka C, Inokawa Y, Hattori N, et al. AMIGO2

- 497 expression as a potential prognostic biomarker for gastric cancer. *Anticancer Res.*
498 2020;40:6713-21. <https://doi.org/10.21873/anticanres.14694>.
- 499 14. Rabenau KE, O'Toole JM, Bassi R, Kotanides H, Witte L, Ludwig DL, et al.
500 DEGA/AMIGO-2, a leucine-rich repeat family member, differentially expressed in
501 human gastric adenocarcinoma: effects on ploidy, chromosomal stability, cell
502 adhesion/migration and tumorigenicity. *Oncogene.* 2004;23:5056–67.
503 <https://doi.org/10.1038/sj.onc.1207681>.
- 504 15. Bi O, Anene CA, Nsengimana J, Shelton M, Roberts R, Newton-Bishop J, Boyne JR.
505 SFPQ promotes an oncogenic transcriptomic state in melanoma. *Oncogene.* 2021;
506 doi:10.1038/s41388-021-01912-4.
- 507 16. Japanese society for cancer of the colon and rectum. Japanese classification of colorectal,
508 appendiceal, and anal carcinoma: the 3d English edition. *J Anus Rectum Colon.*
509 2019;3:175-95. <https://doi.org/10.23922/jarc.2019-018>.
- 510 17. Liu Y, Yang J, Shi Z, Tan X, Jin N, O'Brien C, et al. In vivo selection of highly
511 metastatic human ovarian cancer sublines reveals role for AMIGO2 in intra-peritoneal
512 metastatic regulation. *Cancer Lett.* 2021;503:163-73.
513 <https://doi.org/10.1016/j.canlet.2021.01.024>.
- 514 18. Cui Y, Li C, Jiang Z, Zhang S, Li Q, Liu X, et al. Single-cell transcriptome and genome
515 analyses of pituitary neuroendocrine tumors. *Neuro Oncol.* 2021;00: 00-00.
516 <https://doi.org/10.1093/neuonc/noab102>
- 517 19. Huo T, Canepa R, Sura A, Modave F, Gong Y. Colorectal cancer stages transcriptome
518 analysis. *PLoS One.* 2017;12:e0188697. <https://doi.org/10.1371/journal.pone.0188697>.
- 519 20. Shen S, Gui T, Ma C. Identification of molecular biomarkers for pancreatic cancer with
520 mRMR shortest path method. *Oncotarget.* 2017;8:41432-9.

- 521 <https://doi.org/10.18632/oncotarget.18186>.
- 522 21. Simmen FA, Su Y, Xiao R, Zeng Z, Simmen RCM. The Krüppel-like factor 9 (KLF9)
523 network in HEC-1-A endometrial carcinoma cells suggests the carcinogenic potential of
524 dys-regulated KLF9 expression. *Reprod Biol Endocrinol.* 2008;6:41.
525 <https://doi.org/10.1186/1477-7827-6-41>.
- 526 22. UniProt: The Universal Protein Knowledgebase (UniProt Consortium). 2002.
527 <https://www.uniprot.org/uniprot/Q86SJ2>. Accessed 28 July 2021.
- 528 23. Hefta SA, Paxton RJ, Shively JE. Sequence and glycosylation site identity of two
529 distinct glycoforms of nonspecific cross-reacting antigen as demonstrated by sequence
530 analysis and fast atom bombardment mass spectrometry. *J Biol Chem.*
531 1990;265:8618-26.
- 532 24. Morelle W, Michalski J-C. Analysis of protein glycosylation by mass spectrometry. *Nat*
533 *Protoc.* 2007;2:1585-602. <https://doi.org/10.1038/nprot.2007.227>.
- 534 25. Kim Y-H, O'Neill HM, Whitehead JP. Carboxypeptidase X-1 (CPX-1) is a secreted
535 collagen-binding glycoprotein. *Biochem Biophys Res Commun.* 2015;468:894-9.
536 <https://doi.org/10.1016/j.bbrc.2015.11.053>.
- 537 26. Chen Y, Hor HH, Tang BL. AMIGO is expressed in multiple brain cell types and may
538 regulate dendritic growth and neuronal survival. *J Cell Physiol.* 2012;227:2217-29, 2012.
539 <https://doi.org/10.1002/jcp.22958>.
- 540 27. Moremen KW, Tiemeyer M, Nairn AV. Vertebrate protein glycosylation: Diversity,
541 synthesis and function. *Nat Rev Mol Cell Biol.* 2012;13:448-62.
542 <https://doi.org/10.1038/nrm3383>.
- 543 28. Munkley, J.; Elliott, D.J. Hallmarks of glycosylation in cancer. *Oncotarget.*
544 2016;7:35478-89. <https://doi.org/10.18632/oncotarget.8155>.

- 545 29. Powers TW, Neely BA, Shao Y, Tang H, Troyer DA, Mehta AS, et al. MALDI imaging
546 mass spectrometry profiling of N-glycans in formalin-fixed paraffin embedded clinical
547 tissue blocks and tissue microarrays. PLoS ONE. 2014;9: e106255.
548 <https://doi.org/10.1371/journal.pone.0106255>.
- 549 30. Drake RR, Powers TW, Jones EE, Bruner E, Mehta AS, Angel PM. MALDI mass
550 spectrometry imaging of N-linked glycans in cancer tissues. Adv Cancer Res.
551 2017;134:85-116.
- 552 31. Hill CAS, Farooqui M, Mitcheltree G, Gulbahce HE, Jessurun J, Cao Q, et al. The high
553 affinity selectin glycan ligand C2-O-sLex and mRNA transcripts of the core 2
554 β -1,6-N-acetylglucosaminyltransferase (C2GnT1) gene are highly expressed in human
555 colorectal adenocarcinomas. BMC Cancer. 2009;9:79.
556 <https://doi.org/10.1186/1471-2407-9-79>.
- 557 32. Slawson C, Hart GW. O-GlcNAc signalling: implications for cancer cell biology. Nat
558 Rev Cancer. 2011;11:678-84. <https://doi.org/10.1038/nrc3114>.
- 559 33. Rodriguez E, Schettters STT, Van Kooyk Y. The tumour glyco-code as a novel immune
560 checkpoint for immunotherapy. Nat Rev Immunol. 2018;18:204-11.
561 <https://doi.org/10.1038/nri.2018.3>.
- 562 34. Guan F, Handa K, Hakomori SI. Specific glycosphingolipids mediate
563 epithelial-to-mesenchymal transition of human and mouse epithelial cell lines. Proc Natl
564 Acad Sci USA. 2009;106:7461-6. <https://doi.org/10.1073/pnas.0902368106>.
- 565 35. Häuselmann I, Borsig L. Altered tumor-cell glycosylation promotes metastasis. Front
566 Oncol. 2014;4:28. <https://doi.org/10.3389/fonc.2014.00028>.
- 567 36. Darebna P, Novak P, Kucera R, Topolcan O, Sanda M, Goldman R, et al. Changes in
568 the expression of N- and O-glycopeptides in patients with colorectal cancer and

- 569 hepatocellular carcinoma quantified by full-MS scan FT-ICR and multiple reaction
570 monitoring. *J Proteomics*. 2017;153:44-52. <https://doi.org/10.1016/j.jprot.2016.09.004>.
- 571 37. Nakamori S, Kameyama M, Imaoka S, Furukawa H, Ishikawa O, Sasaki Y, et al.
572 Increased expression of sialyl Lewisx antigen correlates with poor survival in patients
573 with colorectal carcinoma: clinicopathological and immunohistochemical study. *Cancer*
574 *Res*. 1993;53:3632-7.
- 575 38. Hoff SD, Matsushita Y, Ota DM, Cleary KR, Yamori T, Hakomori S, et al. Increased
576 expression of sialyl-dimeric Lex antigen in liver metastases of human colorectal
577 carcinoma. *Cancer Res*. 1989;49:6883-8.
- 578 39. Nakamori S, Kameyama M, Imaoka S, Furukawa H, Ishikawa O, Sasaki Y, et al.
579 Involvement of carbohydrate antigen sialyl Lewis(x) in colorectal cancer metastasis. *Dis*
580 *Colon Rectum*. 1997;40:420-31. <https://doi.org/10.1007/BF02258386>.

581

582 ***Additional File Information***

583 File name: Additional file 1

584 File format: xls

585 Title of data: The monoclonal antibodies with high immunoglobulin titers were selected by
586 enzyme-linked immunosorbent assay (ELISA)

587 Description of data: From December 25, 2017 to January 22, 2018

588

589 ***Figure Legends***

590 **Figure 1**

591 **Specific detection of AMIGO2 by the monoclonal antibody rTNK1A0012**

592 The large membrane was reacted with anti-AMIGO2 antibody, while the small membrane
593 was reacted with an anti- β -actin antibody.

594 A. Cell lysates were prepared from HepG2 cells transfected with human AMIGO1 (A1),
595 AMIGO2 (A2), AMIGO3 (A3), and an empty vector (E). Immunoblotting with
596 rTNK1A0012 (rTNK mAb).

597 B. Immunoblotting with sc-373699 (sc mAb).

598 C. Cell lysates were treated with or without PNGase F and immunoblotted with rTNK
599 mAb.

600 D. Cell lysates were treated with or without alkaline β -elimination and immunoblotted with
601 rTNK mAb.

602

603 **Figure 2**

604 **Detection of three types of AMIGO family molecules by commercially** 605 **available antibodies**

606 A. The same cell lysates as shown in Figure 1 was used. Lysates were prepared from
607 HepG2 cells transfected with human AMIGO1 (A1), AMIGO2 (A2), AMIGO3 (A3),
608 and an empty vector (E). Immunoblotting with LS-C404504 polyclonal antibody.

609 B. Immunoblotting with #36094 polyclonal antibody.

610 C. Immunoblotting with HPA054004 polyclonal antibody.

611

612 **Figure 3**

613 **Immunohistochemical staining for AMIGO2 expression by the monoclonal** 614 **antibody rTNK1A0012 in CRC tissues**

615 AMIGO2 negative expression (A and C) and AMIGO2 high expression (B and D) are
616 shown. Boxed areas in the top row are shown at higher magnification in the bottom row.
617 Scale bars = 400 μm (A and B) and 100 μm (C and D).

618

619 **Figure 4**

620 **Relationship between AMIGO2 expression in primary colorectal cancer**
621 **and metastatic site**

622 A high expression of AMIGO2 was significantly associated with liver metastases (A) and
623 lung metastases (B), but not with peritoneal dissemination (C), as calculated using the X^2
624 test.

625

626 **Figure 5**

627 **Comparison of two AMIGO2 antibodies in AMIGO2 expression and**
628 **survival in CRC patients**

629 Cumulative survival rates were assessed using the Kaplan-Meier plot method. Differences
630 were analyzed using the log-rank test. Overall survival (A) and disease-specific survival
631 (B) are shown.

Figures

Figure 1

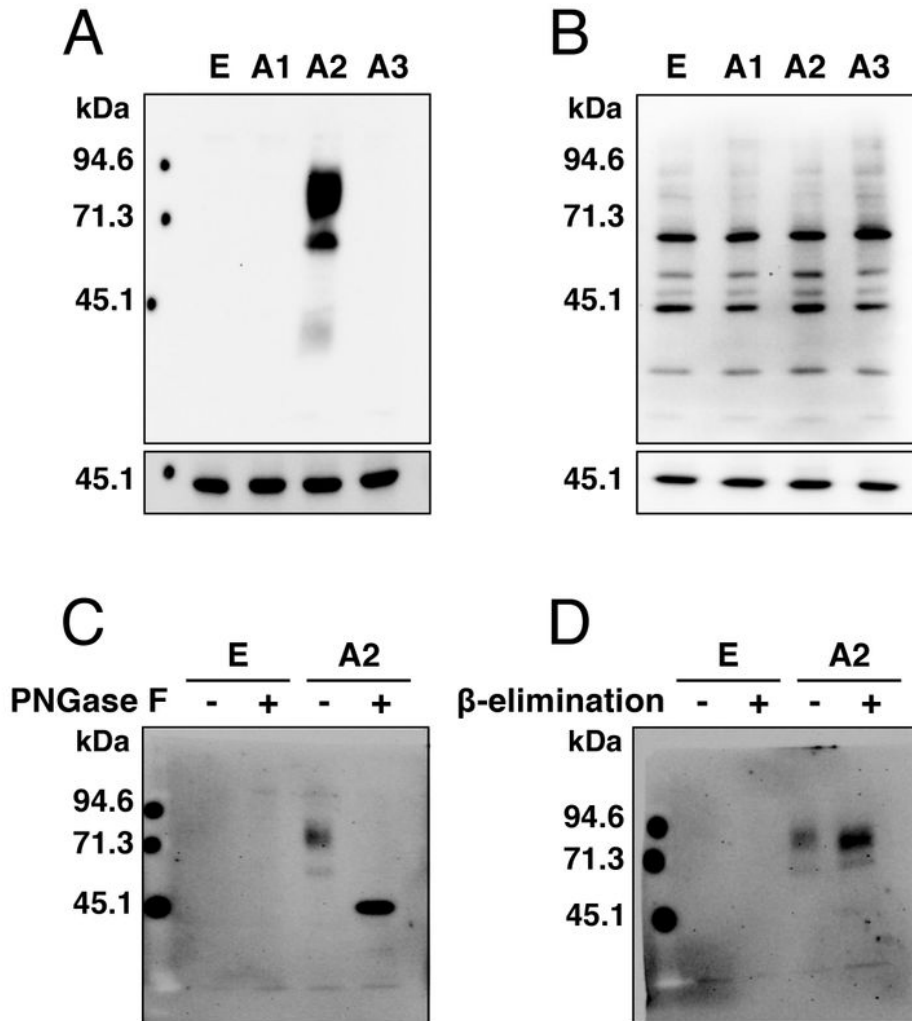


Figure 1

Specific detection of AMIGO2 by the monoclonal antibody rTNK1A0012 The large membrane was reacted with anti-AMIGO2 antibody, while the small membrane was reacted with an anti- β -actin antibody. A. Cell lysates were prepared from HepG2 cells transfected with human AMIGO1 (A1), AMIGO2 (A2), AMIGO3

(A3), and an empty vector (E). Immunoblotting with rTNK1A0012 (rTNK mAb). B. Immunoblotting with sc-373699 (sc mAb). C. Cell lysates were treated with or without PNGase F and immunoblotted with rTNK mAb. D. Cell lysates were treated with or without alkaline β -elimination and immunoblotted with rTNK mAb.

Figure 2

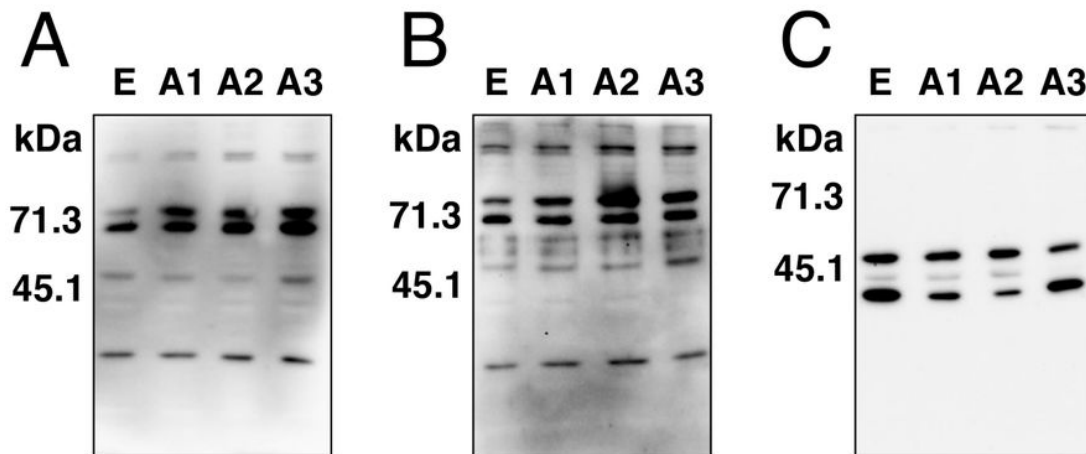


Figure 2

Detection of three types of AMIGO family molecules by commercially available antibodies A. The same cell lysates as shown in Figure 1 was used. Lysates were prepared from HepG2 cells transfected with human AMIGO1 (A1), AMIGO2 (A2), AMIGO3 (A3), and an empty vector (E). Immunoblotting with LS-C404504 polyclonal antibody. B. Immunoblotting with #36094 polyclonal antibody. C. Immunoblotting with HPA054004 polyclonal antibody.

Figure 3

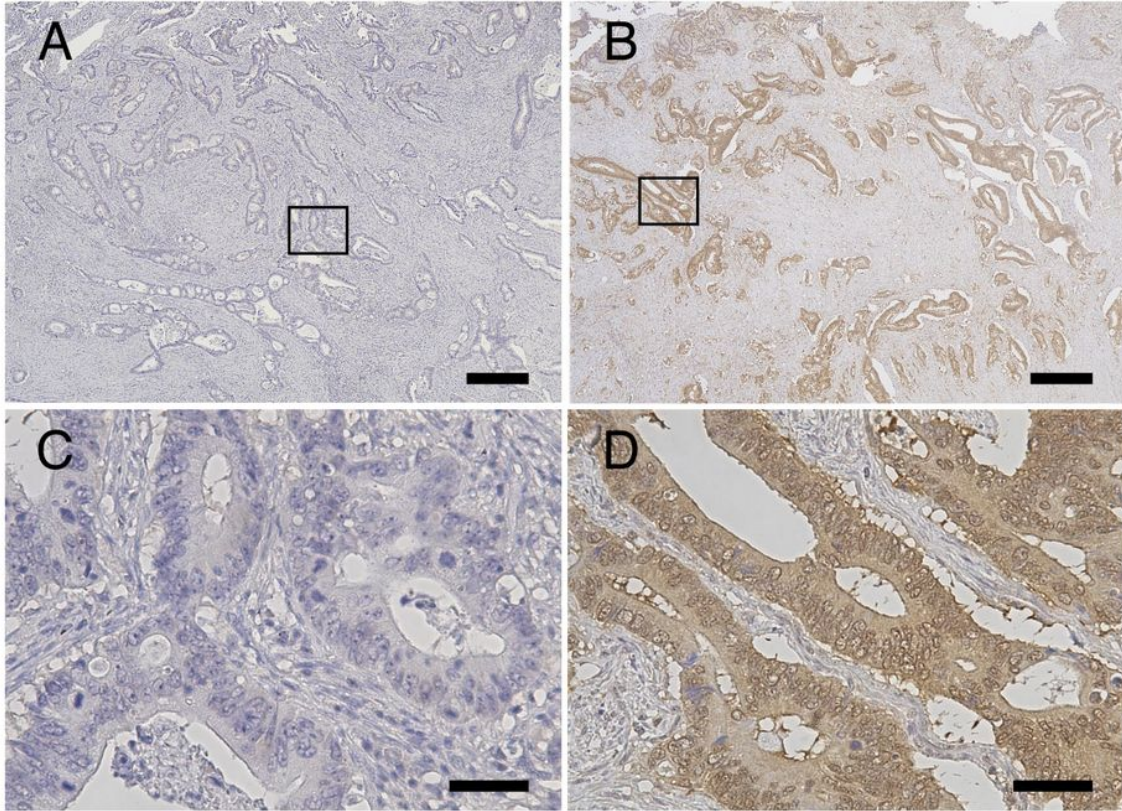


Figure 3

Immunohistochemical staining for AMIGO2 expression by the monoclonal antibody rTNK1A0012 in CRC tissues AMIGO2 negative expression (A and C) and AMIGO2 high expression (B and D) are shown. Boxed areas in the top row are shown at higher magnification in the bottom row. Scale bars = 400 μm (A and B) and 100 μm (C and D).

Figure 4

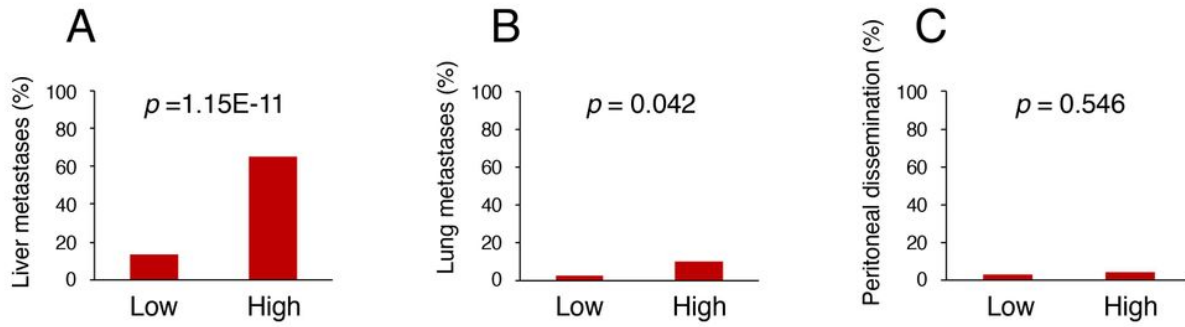


Figure 4

Relationship between AMIGO2 expression in primary colorectal cancer and metastatic site A high expression of AMIGO2 was significantly associated with liver metastases (A) and lung metastases (B), but not with peritoneal dissemination (C), as calculated using the X2 test.

Figure 5

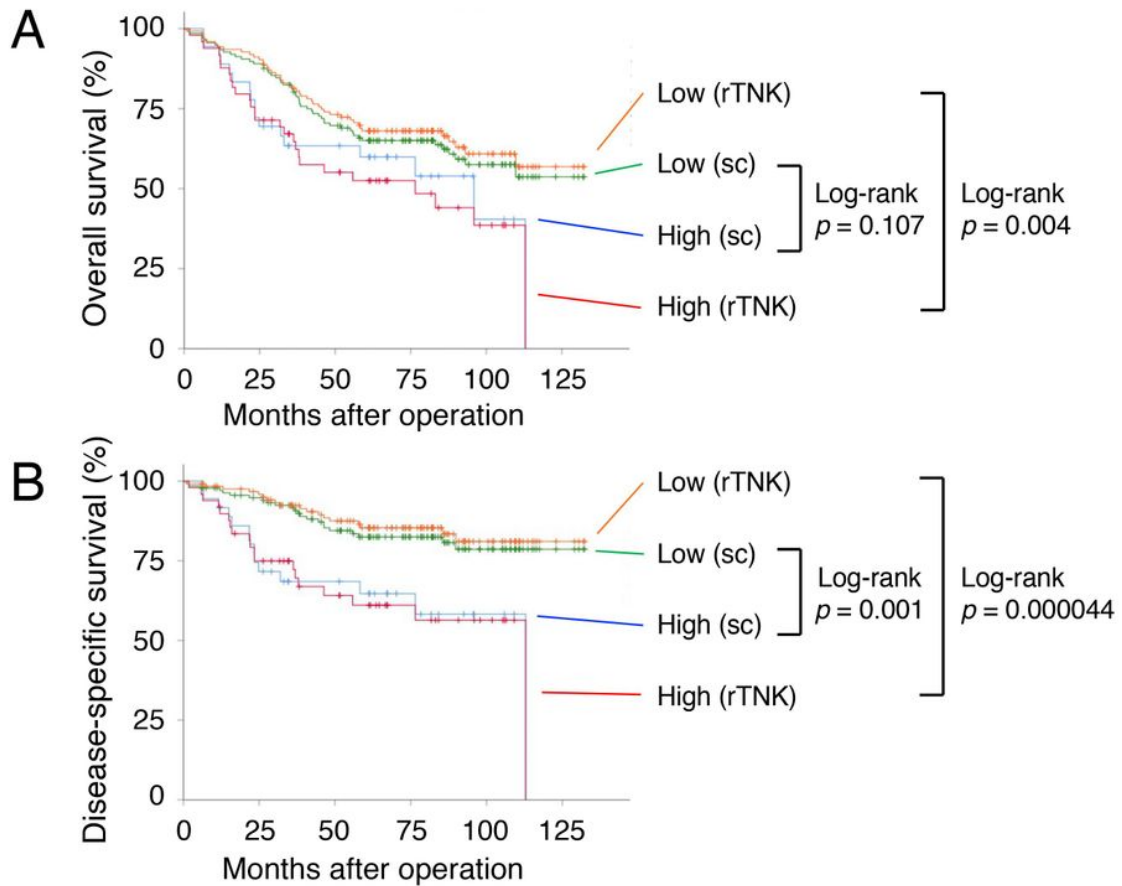


Figure 5

Comparison of two AMIGO2 antibodies in AMIGO2 expression and survival in CRC patients. Cumulative survival rates were assessed using the Kaplan-Meier plot method. Differences were analyzed using the log-rank test. Overall survival (A) and disease-specific survival (B) are shown.

Supplementary Files

This is a list of supplementary files associated with this preprint. Click to download.

- [AdditionalFile1.pdf](#)
- [Table1.pdf](#)
- [Table2.pdf](#)
- [Table3.pdf](#)